Supplement of Hydrol. Earth Syst. Sci., 24, 1763–1779, 2020
https://doi.org/10.5194/hess-24-1763-2020-supplement

Hydrology and Earth System Sciences
Open Access

Supplement of

Using Gravity Recovery and Climate Experiment data to derive corrections to precipitation data sets and improve modelled snow mass at high latitudes

Emma L. Robinson and Douglas B. Clark

Correspondence to: Emma L. Robinson (emrobi@ceh.ac.uk)

1 Meteorology

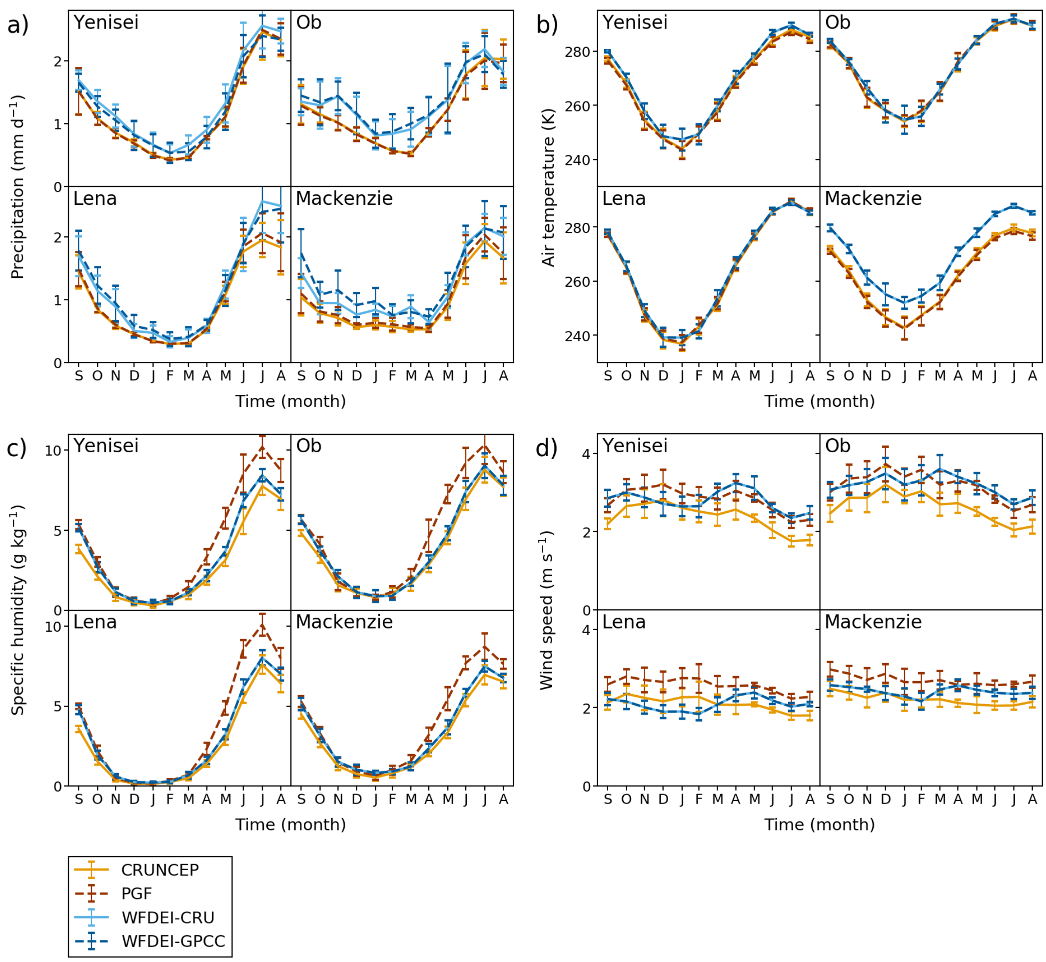

Figure S1: Mean-monthly climatology of meteorological variables in each driving data set, averaged over the common overlap period, 2002–2010. (a) Precipitation (mm d^{-1}), (b) Near surface air temperature (K), (c) Specific humidity (g kg^{-1}), (d) Wind speed at 10 m (m s^{-1}). Error bars show the standard deviation. The precipitation differs significantly between the data sets with and without undercatch correction. In general, the air temperature is very similar between data sets, except in the Mackenzie. The specific humidity is much higher in the PGF data than in the other data sets. The wind speed is variable between data sets in all basins.

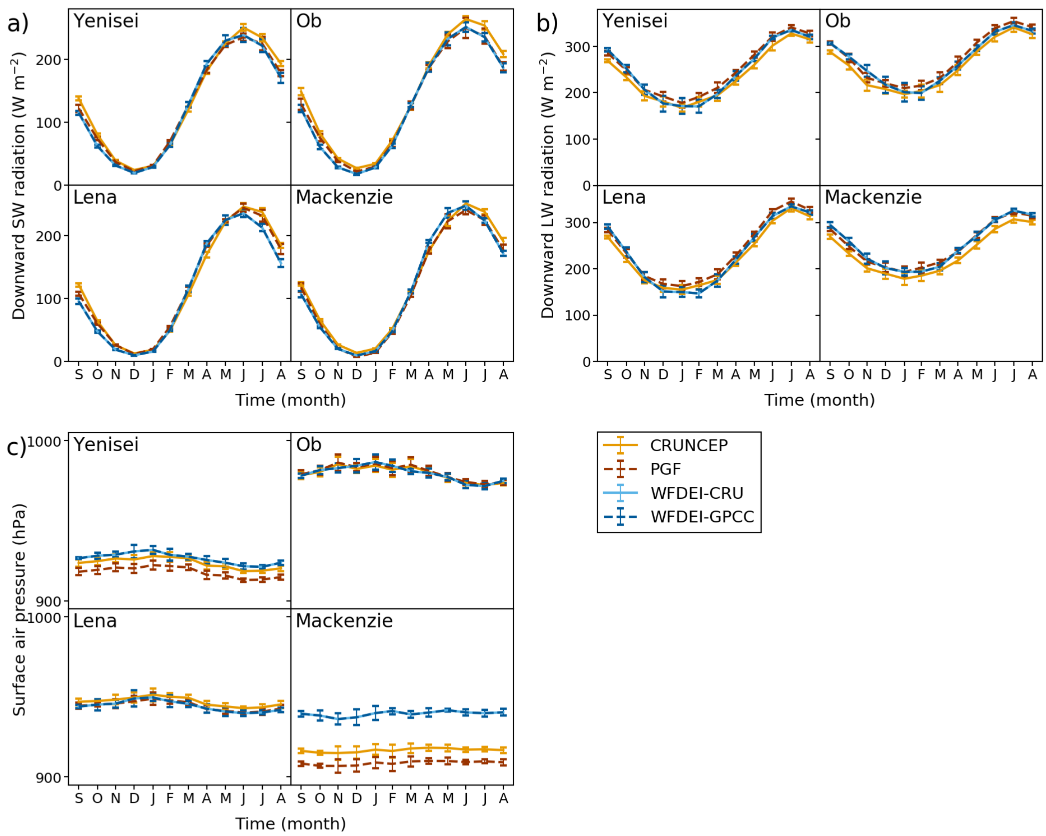

Figure S2: Mean-monthly climatology of meteorological variables in each driving data set, averaged over the common overlap period, 2002–2010. (a) Downward shortwave radiation (W m^{-2}), (b) Downward longwave radiation (W m^{-2}), (c) Surface air pressure (hPa). Error bars show the standard deviation. The radiation variables are both quite consistent between data sets. The surface air pressure is most variable in the Mackenzie and the Yenisei, and more consistent in the Lena and Ob.

2 Precipitation

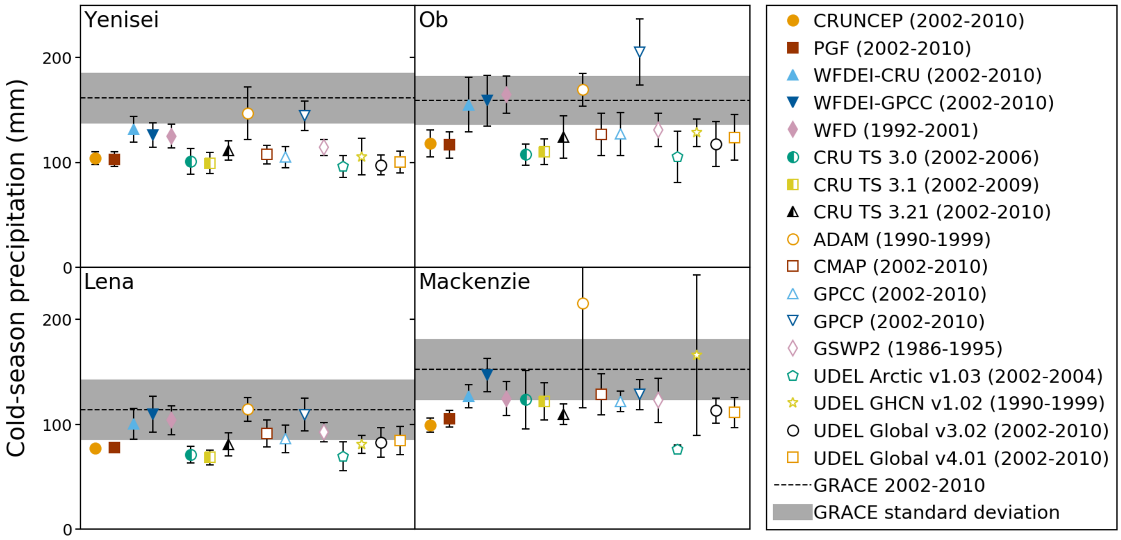

Figure S3: Mean cold season (October – February) precipitation calculated from several gridded, observation-based data sets. Where the data are available, the means are calculated over the nine-year common overlap period used in this study, 2002–2010. If the data partially overlap with this period, then the years of overlap are used. Otherwise, the last nine years of the data set are used. Years used for each data set are noted in the legend. The first four data sets are the driving data used in this study [1, 2, 3], the fifth, WFD [4], is the precursor to the WFDEI data sets. The next three are three different versions of CRU TS [5]. Two of these (3.1 and 3.21) have been used in bias-correcting the driving data used in this study. The rest are precipitation data from a variety of sources (ADAM [6], CMAP [7, 8], GPCC v7 [9, 10], GPCP v2.2 [11], GSWP2 [12], UDEL [13, 14, 15, 16]). Earlier versions (v5 and v6) of the GPCC data set were used to bias-correct the WFDEI-GPCC driving data. The black dashed line shows the mean cold season precipitation calculated using the GRACE-based water balance (Section 4.1), with the shaded grey area showing the standard deviation. In general, most of the data sets lie below the GRACE estimate. Some, notably the WFDEI driving data, which include undercatch correction, are much closer to the GRACE mean, but still tend to underestimate overall, while a few significantly overestimate.

3 Basin fluxes

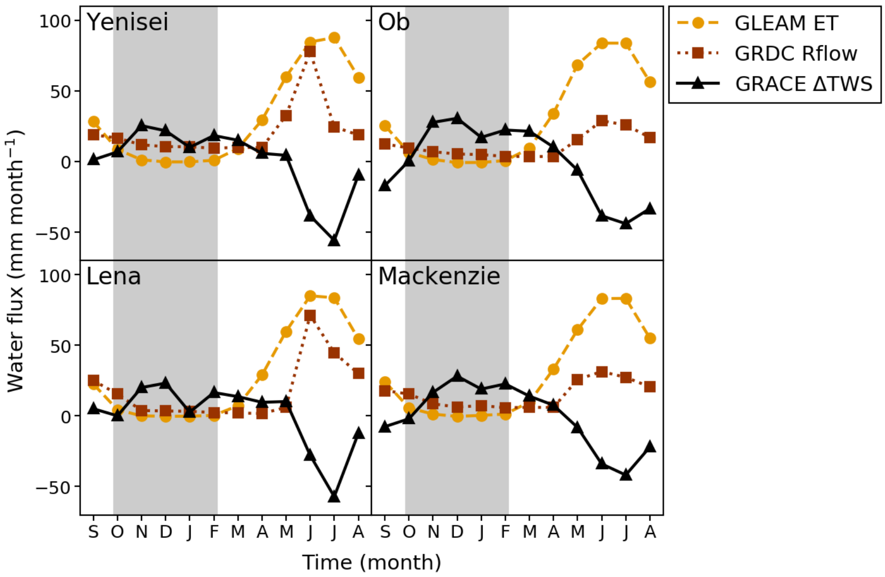

Figure S4: Mean-monthly climatology of the fluxes used to calculate the inferred precipitation (GLEAM evapotranspiration, GRDC basin discharge and change in GRACE total water storage (TWS)) for the common overlap period, 2002–2010. The grey shaded area shows the months (October – February inclusive) which are considered when calculating the cold season precipitation. In these months the relative sizes of the evaporation and basin discharge are similar to or smaller than the change in TWS estimated by GRACE. Outside of these months, the calculation is dominated by the evaporation and basin discharge, so their uncertainties would have more impact.

4 Snow water equivalent (SWE)

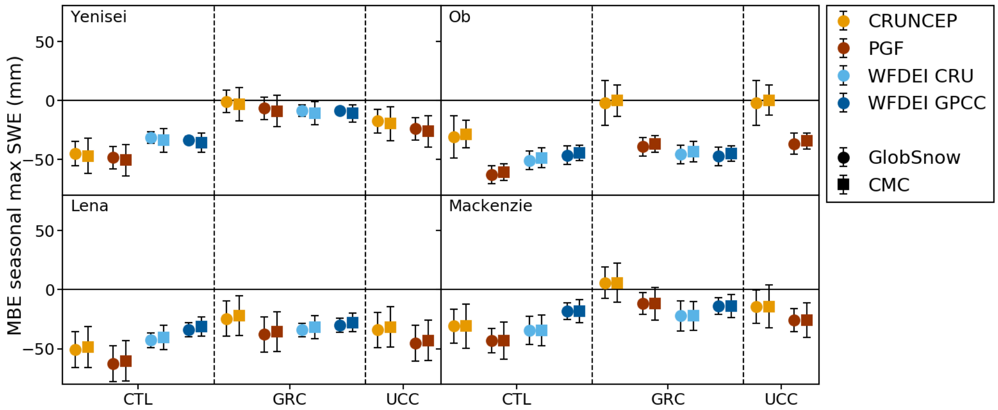

Figure S5: Mean bias error (MBE) of seasonal maximum SWE (mm), calculated for each basin over the common overlap period, 2002–2010. The error bars show the standard deviation, σ_b (Eq. 3). The improvement in the MBE in the GRC and UCC runs varies between basins (the Yenisei and Mackenzie are most improved) and between data sets (CRUNCEP is most improved in all basins).

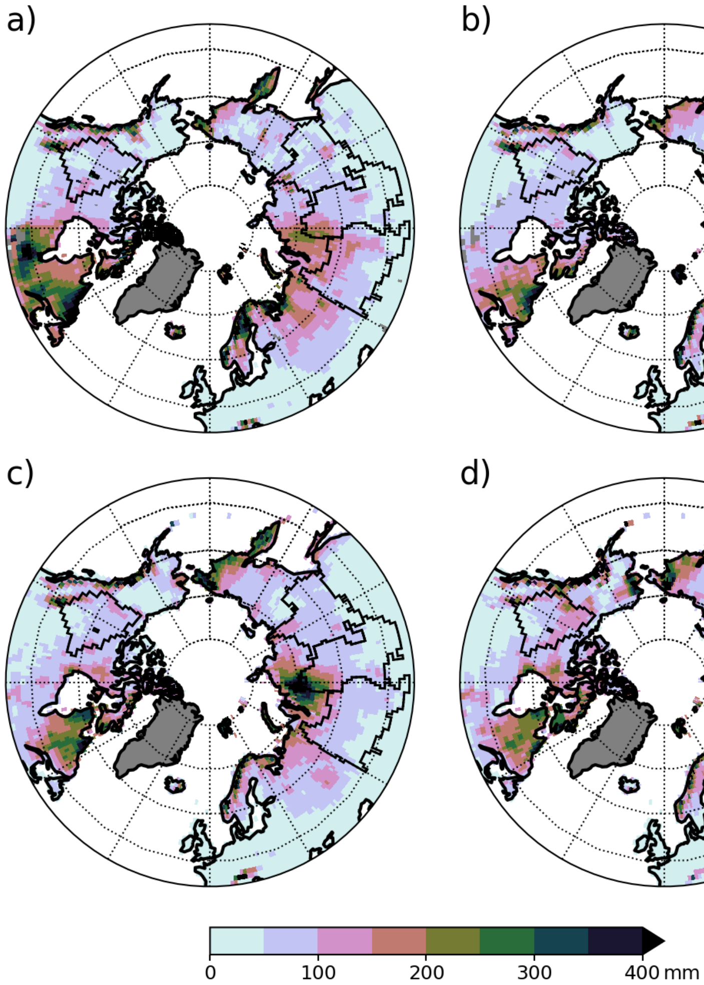

Figure S6: Modelled seasonal maximum SWE (mm), CTL runs for the common overlap period, 2002–2010. (a) CRUNCEP, (b) PGF, (c) WFDEI-CRU, (d) WFDEI-GPCC.

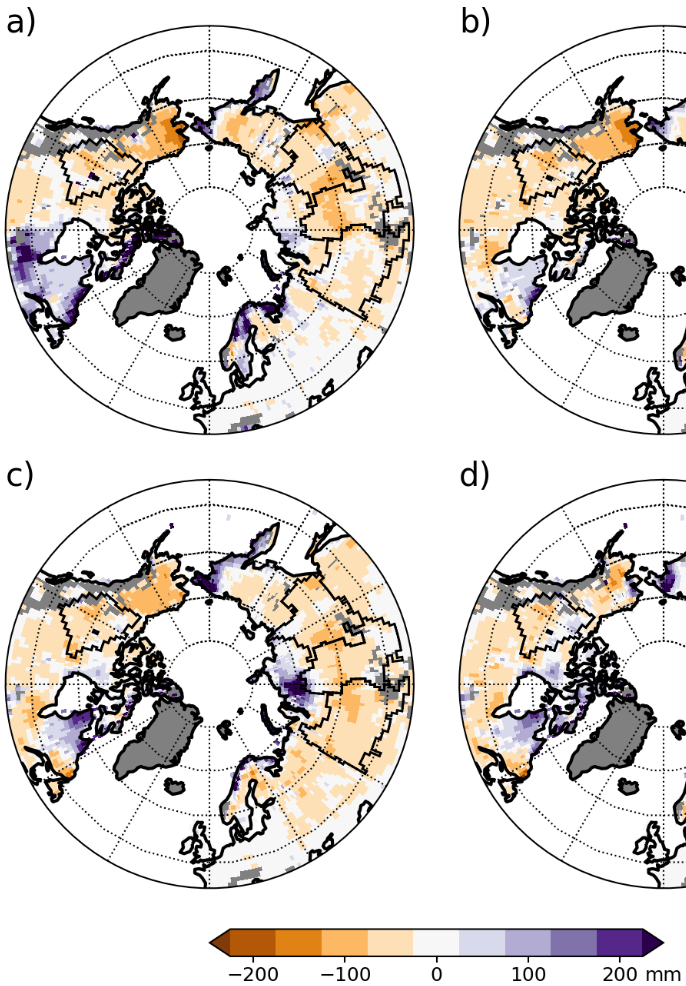

Figure S7: Difference modelled (CTL runs) and observed (GlobSnow) seasonal maximum SWE (mm) for the common overlap period, 2002–2010. (a) CRUNCEP, (b) PGF, (c) WFDEI-CRU, (d) WFDEI-GPCC. Although there are some regions where the SWE is overestimated, in general the seasonal maximum SWE in each basin is underestimated compared with both GlobSnow and CMC.

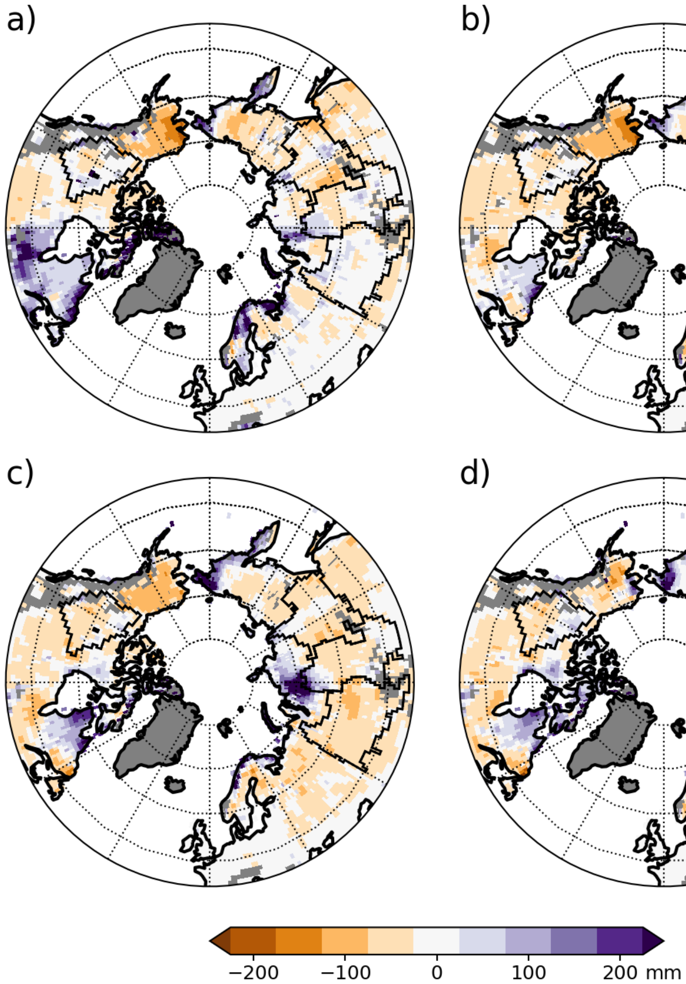

Figure S8: Difference between modelled (GRC runs) and observed (GlobSnow) seasonal maximum SWE (mm) for the common overlap period, 2002–2010. (a) CRUNCEP, (b) PGF, (c) WFDEI-CRU, (d) WFDEI-GPCC. Although there is still a general underestimation of SWE, the bias is reduced, and there are more regions of close agreement or overestimation.

5 Basin discharge

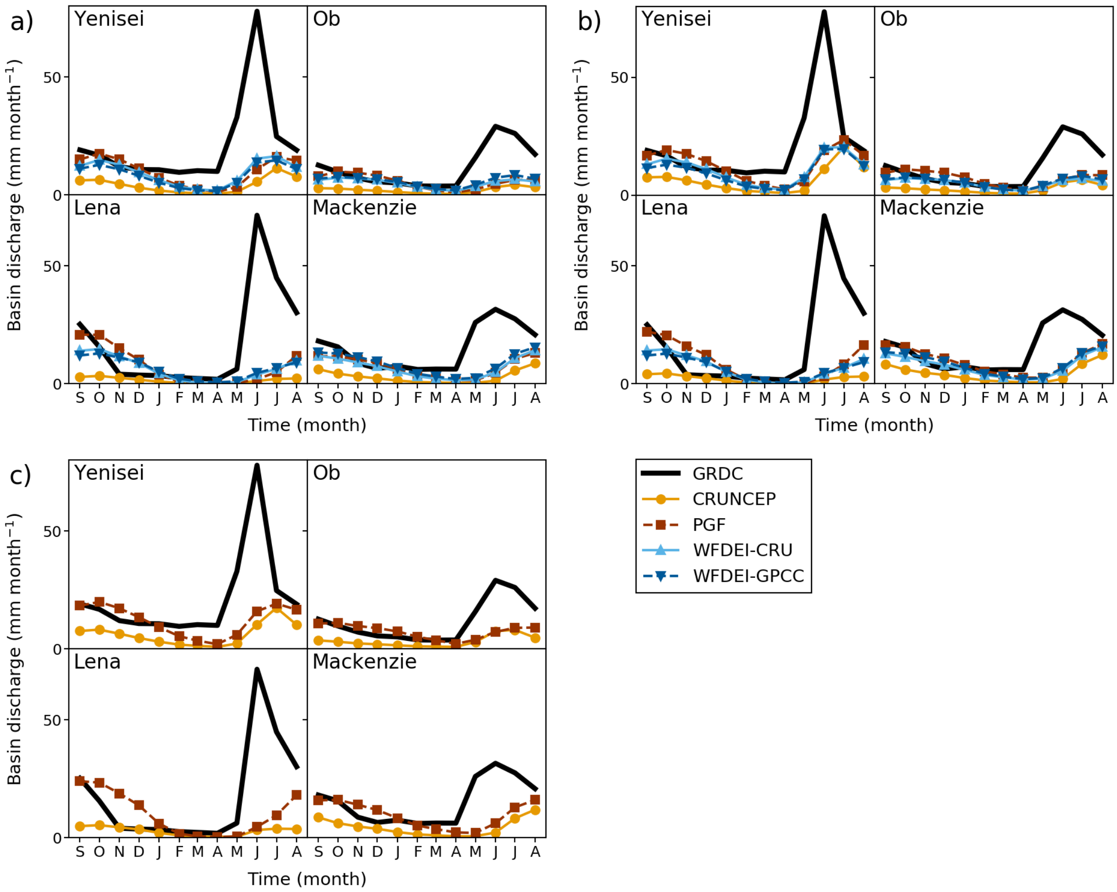

Figure S9: Mean-monthly climatology of basin discharge (mm month^{-1}) for (a) CTL runs, (b) GRC runs and (c) UCC runs, averaged over the common overlap period, 2002–2010. JULES fails to reproduce the timing and magnitude of the spring peak.

6 Water balance

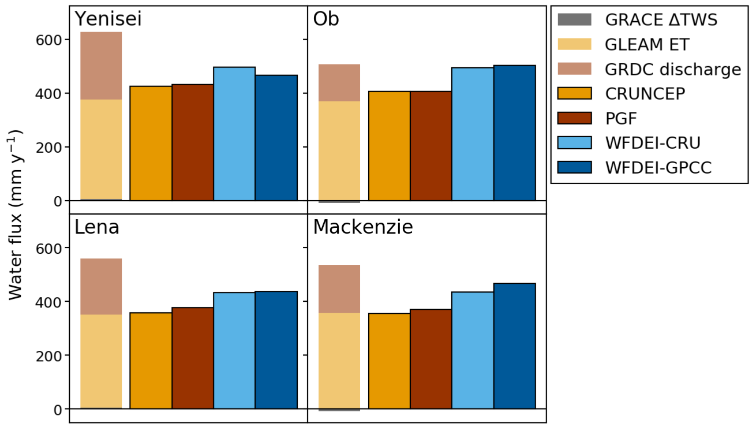

Figure S10: Annual water balance (mm y^{-1}) calculated from the observed products used in this study, compared with the annual precipitation in each of the precipitation data sets (mm y^{-1}), for 2002–2010. The left-most bar combines the annual mean GRDC discharge, GLEAM evapotranspiration and the GRACE change in total water storage (ΔTWS) which is a small term, following Eq. 5, giving an estimate of the total water input into each basin. On the annual scale, this is dominated by evapotranspiration and river flow. This input is notably larger than the precipitation in the study data sets, consistent with the idea that there is insufficient precipitation in these data sets.

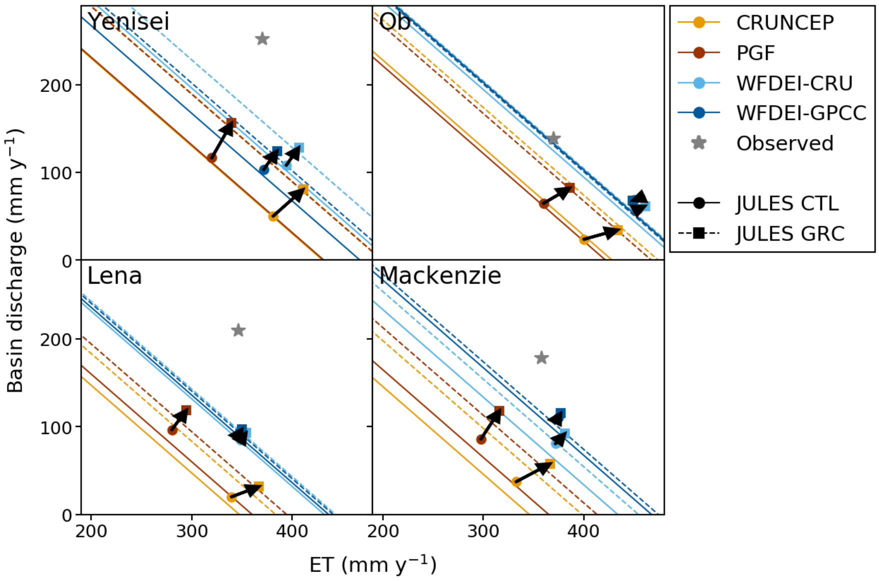

Figure S11: Annual basin discharge (mm y^{-1}) against annual evaporation flux (mm) for CTL and GRC runs 2002–2010. Lines show the precipitation limit (mm y^{-1}). Note that, although the x- and y-axis limits differ, the scales are the same, such that a unit change on one axis is the same length as a unit change on the other. The evaporation is several times larger than the basin discharge. The arrows show the direction of change between the CTL and GRC runs. A more vertical arrow shows that the increased cold season precipitation causes more increase in basin discharge (eg. PGF runs), while a more vertical arrow shows that the increase is more in the evaporation (eg. CRUNCEP runs).

7 Sensitivity test: scaling precipitation throughout the year

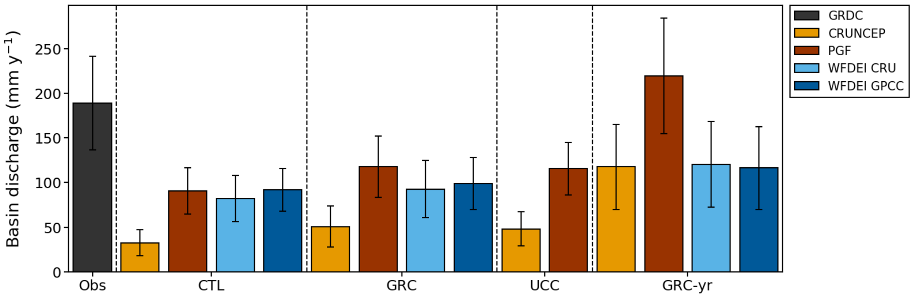

Figure S12: Mean annual observed and modelled basin discharge (mm y^{-1}) for the common overlap period, 2002–2010. This figure repeats Fig. 5 from the main text, but adds a final panel to show the results of a sensitivity test, in which the scale factors derived from the cold season were applied to the precipitation throughout the whole year (GRC-yr). This mostly results in an increase in summer rainfall, and a doubling of the basin discharge in CRUNCEP and PGF. After applying this increase in precipitation, the PGF discharge is much closer to the observed. CRUNCEP is still low compared to observations, but this may be partially explained by the higher rainfall interception, The increases in WFDEI-CRU and WFDEI-GPCC are more modest, since the cold-season scale factors are smaller. due to a longer timestep in the driving data. This sensitivity test suggests, that all of the precipitation data sets considered in this study may benefit from an increase in precipitation outside of the cold season.

8 Information about data sets and model runs

Table S1: GRDC data availability and use. The mean-monthly climatology was calculated over all the available data, then missing months and years gap-filled with this climatology.

Basin	Years available	Months missing	Years replaced with climatology
Yenisei	1936–2011		2012–2017
Ob	1930–2010	2000 (whole year)	2011–2017
Lena	1951–2002		2003–2017
Mackenzie	1972–2011	1972 (Jan, Feb, Apr, Jun) 1997 (Nov, Dec) 1998 (Jan, Feb, Mar)	2012–2017

Table S2: Rose suite IDs and revisions for each experiment. All are available from the repository at `https://code.metoffice.gov.uk/trac/roses-u` or through the browser at `https://code.metoffice.gov.uk/rosie/u` (registration required).

Experiment	Driving data	Rose id	Revision
CTL	CRUNCEP	u-at900	70155
	PGF	u-bb972	93780
	WFDEI-CRU	u-ao929	70151
	WFDEI-GPCC	u-av156	70158
GRC	CRUNCEP	u-aw333	85408
	PGF	u-bc394	94656
	WFDEI-CRU	u-aw349	85554
	WFDEI-GPCC	u-aw347	85494
UCC	CRUNCEP	u-av896	71361
	PGF	u-bc419	94745

References

[1] Nicolas Viovy. CRUNCEP v4 (CRU TS 3.21), 2014. URL `https://dods.extra.cea.fr/store/p529viov/cruncep/V4_1901_2012`. Accessed: 2014-07-11.

[2] Justin Sheffield, Gopi Goteti, and Eric F. Wood. Development of a 50-year high-resolution global dataset of meteorological forcings for land surface modeling. *Journal of Climate*, 19(13):3088–3111, 2006. doi:10.1175/JCLI3790.1.

[3] Graham P. Weedon, Gianpaolo Balsamo, Nicolas Bellouin, Sandra Gomes, Martin J. Best, and Pedro Viterbo. The WFDEI meteorological forcing data set: WATCH Forcing Data methodology applied to ERA-Interim reanalysis data. *Water Resources Research*, 50(9):7505–7514, 2014. doi:10.1002/2014WR015638.

[4] G. P. Weedon, S. Gomes, P. Viterbo, W. J. Shuttleworth, E. Blyth, H. Österle, J. C. Adam, N. Bellouin, O. Boucher, and M. Best. Creation of the WATCH Forcing Data and its use to assess global and regional reference crop evaporation over land during the twentieth century. *Journal of Hydrometeorology*, 12(5):823–848, 2011. doi:10.1175/2011JHM1369.1.

[5] I. Harris, P.D. Jones, T.J. Osborn, and D.H. Lister. Updated high-resolution grids of monthly climatic observations – the CRU TS3.10 Dataset. *International Journal of Climatology*, 34(3):623–642, 2013. doi:10.1002/joc.3711.

[6] Jennifer C. Adam, Elizabeth A. Clark, Dennis P. Lettenmaier, and Eric F. Wood. Correction of global precipitation products for orographic effects. *Journal of Climate*, 19(1):15–38, 2006. doi:10.1175/JCLI3604.1.

[7] Pingping Xie and Phillip A. Arkin. Global Precipitation: A 17-year monthly analysis based on gauge observations, satellite estimates, and numerical model outputs. *Bulletin of the American Meteorological Society*, 78(11):2539–2558, 1997. doi:10.1175/1520-0477(1997)078<2539:GPAYMA>2.0.CO;2.

[8] NOAA/OAR/ESRL PSD. CMAP Precipitation data, 2018. URL `https://www.esrl.noaa.gov/psd/data/gridded/data.cmap.html`. NOAA/OAR/ESRL PSD, Boulder, Colorado, USA. Accessed: 2018-01-05.

[9] Udo Schneider, Andreas Becker, Peter Finger, Anja Meyer-Christoffer, Markus Ziese, and Bruno Rudolf. GPCC's new land surface precipitation climatology based on quality-controlled in situ data and its role in quantifying the global water cycle. *Theoretical and Applied Climatology*, 115(1): 15–40, Jan 2014. ISSN 1434-4483. doi:10.1007/s00704-013-0860-x.

[10] Udo Schneider, Andreas Becker, Peter Finger, Anja Meyer-Christoffer, Bruno Rudolf, and Markus Ziese. GPCC Full Data Monthly Product Version 7.0 at 1.0°: Monthly land-surface precipitation from rain-gauges built on GTS-based and historic data, 2015. URL `https://opendata.dwd.de/climate_environment/GPCC/html/fulldata_v7_doi_download.html`. Global Precipitation Climatology Centre (GPCC, http://gpcc.dwd.de/) at Deutscher Wetterdienst. Accessed: 2018-02-07.

[11] G.J. Huffman, D.T. Bolvin, and R.F. Adler. GPCP Version 2.2 SG Combined Precipitation Data Set, 2012. URL `http://www.ncdc.noaa.gov/oa/wmo/wdcamet-ncdc.html`. WDC-A, NCDC, Asheville, NC. Accessed: 2018-02-07.

[12] Paul A. Dirmeyer, Xiang Gao, Mei Zhao, Zhichang Guo, Taikan Oki, and Naota Hanasaki. GSWP-2: Multimodel analysis and implications for our perception of the land surface. *Bulletin of the American Meteorological Society*, 87(10):1381–1398, 2006. doi:10.1175/BAMS-87-10-1381.

[13] Kenji Matsura and Cort J. Willmott. Arctic land-surface precipitation: 1930-2004 gridded monthly time series, 2005. URL http://climate.geog.udel.edu/~climate/html_pages/Arctic4_files/README.arctic.p_ts4.html. Accessed 2006-01-04.

[14] Cort J. Willmott and Kenji Matsura. Terrestrial air temperature and precipitation: Monthly and annual time series (1950 - 1999), 2001. URL http://climate.geog.udel.edu/~climate/html_pages/README.ghcn_ts2.html. Accessed 2001-11-06.

[15] Kenji Matsura and Cort J. Willmott. Terrestrial precipitation: 1900-2010 gridded monthly time series, 2012. URL http://climate.geog.udel.edu/~climate/html_pages/Global2011/Precip_revised_3.02/README.GlobalTsP2011.html. Accessed 2013-01-21.

[16] Kenji Matsura and Cort J. Willmott. Terrestrial precipitation: 1900-2014 gridded monthly time series, 2015. URL http://climate.geog.udel.edu/~climate/html_pages/Global2014/README.GlobalTsP2014.html. Accessed 2015-03-16.